Organic Electronics 41 (2017) 1–8

Contents lists available at ScienceDirect

Organic Electronics

journal homepage: www.elsevier.com/locate/orgel

Benzothiadiazole-pyrrolo[3,4-*b*]dithieno[2,3-*f*:3′,2′-*h*] quinoxalindione-based random terpolymer incorporating strong and weak electron accepting [1,2,5]thiadiazolo[3,4*g*]quinoxalinefor polymer solar cells

M.L. Keshtov [a, **], A.R. Khokhlov [a], S.A. Kuklin [a], S.A. Osipov [a], N.A. Radychev [b], M.I. Buzin [a], Ganesh D. Sharma [c, *]

[a] Institute of Organoelement Compounds of the Russian Academy of Sciences, Vavilova St., 28, 119991, Moscow, Russian Federation
[b] Carl von Ossietzky University of Oldenburg, 26129, Oldenburg, Germany
[c] Department of Physics, The LNM Institute for Information Technology, Jamdoli, Jaipur, Rajasthan 302031, India

ARTICLE INFO

Article history:
Received 12 October 2016
Received in revised form
4 November 2016
Accepted 23 November 2016
Available online 2 December 2016

Keywords:
D-A random copolymers
Bulk heterojunction
Polymer solar cells
Solvent additives
Power conversion efficiency

ABSTRACT

We report the synthesis of a D-A random terpolymer denoted as **P2** consists of one thiophene donor unit and three acceptor benzothiadiazole (BT), pyrrolodithienoquinoxalinedione (PDQD) and thiadiazoloquinoxaline (TDQ) units by Stille-coupling reaction and investigated its optical and electrochemical properties. We have compared its properties with the parent copolymer **P1**. The **P2** exhibits bandgap of about 1.18 eV which is lower than that of **P1** (1.50 eV), indicating strength of accepting units controls both the optical and electrochemical bandgap. We have used terpolymer **P2** as electron donor along with [6,6]-phenyl C_{71} butyric acid methyl ester ($PC_{71}BM$) as electron acceptor for the fabrication of solution processed bulk heterojunction polymer solar cells (PSCs). PSC based on an optimized **P2**:$PC_{71}BM$ (1:2 by weight) active layer processed with 3v % DIO/DCB solution, displayed a power conversion efficiency (PCE) of 7.22%, which is higher than that for **P1** based polymer solar cell (PCE = 6.56%) processed under same conditions. The higher value of PCE for **P2**:$PC_{71}BM$ may be related to more favorable phase separated morphology of active layer as compared to **P1**:$PC_{71}BM$, beneficial for the exciton dissociation and charge transport, as evidenced from the larger hole mobility.

1. Introduction

Polymer solar cells (PSCs) based on bulk heterojunction (BHJ) active layer that consist of a blended film of a conjugated polymer donor and fullerene derivatives acceptor have attracted lot of attention as a promising renewable energy resource due to their unique advantages for achieving light weight, low cost, large area and flexible devices through inject printing and roll to roll solution processes [1]. Significant progress in the field of PSCs has been made in past few years and has shown power conversion efficiencies (PCEs) over 10% using conjugated polymers as donor and fullerene derivatives as acceptor in single BHJ junction devices, particularly due to the optimization of bandgap, charge carrier mobility and energy levels of conjugated polymers, and the nanoscale morphology of the active layer [2]. However, further development of conjugated polymers is necessary to achieve high performance PSCs for commercialization [3]. One promising approach toward the broadening of absorption profile of polymers is to develop random terpolymers based on the copolymerization of two different electron rich units and one electron deficient unit [4] or one electron rich unit and two different electron withdrawing units [5]. Moreover, the energy levels, absorption profile, molecular ordering and charge carrier mobility can be adjusted by controlling the selection of different monomers or the ratio of composition [6]. Moreover, the choice of co-monomers with planar molecular structure can also enhance the π-π interaction between copolymer chain backbones. Ternary copolymerization is an easy and effective method used to tune the optical and electronic properties of the conjugated copolymers and the PCE of the resultant devices can be

* Corresponding author.
** Corresponding author.
E-mail addresses: sharmagd_in@yahoo.com, gsharma273@gmail.com (G.D. Sharma).

http://dx.doi.org/10.1016/j.orgel.2016.11.034
1566-1199/

enhanced as compared to D-A copolymer counterpart. Tajima and coworker reported a terpolymer based on BDT, TPD and thiophene and the thiophene unit has a tris-(thienylenevinylene) conjugated side chain and achieved PCE of 6.46%, higher than that for D-A copolymer [7]. Recently Jo et al. synthesized a conjugated random copolymer composed of bithiophene (electron donating unit) with thiophene-capped diketopyrrolopyrrole (TDPP) and pyridine-capped diketopyrrolopyrrole (PyDPP) (co-electron accepting units) and employed it as electron donor along with $PC_{71}BM$ as electron acceptor for BHJ PSC, achieved overall PCE of 8.11% [8]. Na et al. have reported a new random terpolymer based on (2,5-difluorophenylene) dithiophene and dialkoxybenzothiadiazole with thiophene as the third conjugated bridge having sulfur and fluorine (S/F) and/or oxygen (S/O) non-covalent intramolecular interaction and reported overall PCE of 7.71% and 8.50% for conventional and inverted PSCs, respectively [9]. These observations indicate that a rational selection of the three components and detail characterization of the molecular structure with multiple components is crucial for the designing of new terpolymers for efficient PSCs.

In our recent work [10] we prepared D-A copolymer **P1** (chemical structure shown in Scheme 1), which exhibited promising optical and electrochemical properties. In order to further improve the characteristics of the parent polymer **P1** we developed new random terpolymer **P2** comprising additional electron acceptors with different electron withdrawing ability, units **M3** (strong acceptor). Our study clearly shows that introduction of additional strong acceptor unit **M3** leads to broaden and red-shifted absorption spectrum of **P2** compared to parent copolymer **P1**. Random terpolymer **P2** was used as electron donor along with the $PC_{71}BM$ as electron acceptor for the fabrication of solution processed BHJ PSCs. After the optimization of donor to acceptor ratio and solvent additive concentration, the device based on **P2**:$PC_{71}BM$ showed overall PCE of 7.22%, higher than that for **P1** based solar cells processed under same fabrication conditions [10]. The higher value of PCE for **P2**:$PC_{71}BM$ may be related to more favorable phase separated morphology of active layer as compared to **P1**:$PC_{71}BM$, beneficial for the exciton dissociation and charge transport, as evidenced from the larger hole mobility. Moreover, a high PCE of 7.22% is achieved with low energy loss (0.46 eV) with a low bandgap random terpolymer **P2** (1.18 eV), which may be the highest PCE with our best of knowledge.

2. Experimental details

^1H NMR and ^{13}C NMR spectra were measured with Bruker AVANCE 400 spectrometer. UV–vis spectra were measured on Perkin Elmer Lamada-25 spectrometer. The elemental analysis was performed with an Elementar Vario EL III element analyzer for C, H, N and S determination. Thermal gravimetric analysis (TGA) analysis was performed on "Perkin-Elmer TGA-7″ with heating rate 20 deg/min. The average molecular weight and poly-dispersity index (PDI) of the copolymers was performed on Waters gel permeation chromatography GPC instrument, consisting of a M-600 pump, two U-Styragel Linear Columns, M-484 spectrophotometric detector and maxima data acquisition and processing system with $CHCl_3$ as eluent and polystyrene as standard. Electrochemical redox potentials were obtained by cyclic voltammetry (CV) using a three-electrode cell and an electrochemistry work station (CHI830B, Chenhua Shanghai). The working electrode was a Pt ring electrode; the auxiliary electrode was a Pt wire, and Ag/AgCl was used as reference electrode. The *tetra*-butylammoniumhexafluorophosphate 0.1 M was used as supporting electrolyte in dry acetonitrile. Transmission electron microscopy (TEM) images were recorded with a Tecnai G2F30 transmission electron microscope (FEI Inc.; accelerating voltage = 300 kV).

3. Synthesis of random terpolymers P2

Toluene was dried and distilled over sodium/benzophenone. $CHCl_3$ and CH_3CN were dried with CaH_2 and distilled prior to use. All other solvents and chemicals used in this work were analytical grade and used without further purification. All chromatographic separations were carried out on silica gel (200–300 mesh).

The polymerization was performed by a Stille coupling reaction. In a 50 mL flask, monomers **M1** (0.3130 g, 0.5 mmol), **M2** (0.1874 g, 0.25 mmol) and **M3** (0.1836 g, 0.25 mmol) were dissolved in 15 mL of toluene, and the solution was flushed with argon for 15 min, then 27 mg of $Pd(PPh_3)_4$ was added into the solution. The mixture was again flushed with argon for 20 min. The reaction mixture was heated to reflux for 48 h. The reaction mixture was cooled to room temperature and added drop-wise to 400 mL methanol. The precipitate was collected and further purified by Soxhlet extraction with methanol, hexane, and chloroform in sequence. The chloroform fraction was concentrated and added drop-wise into

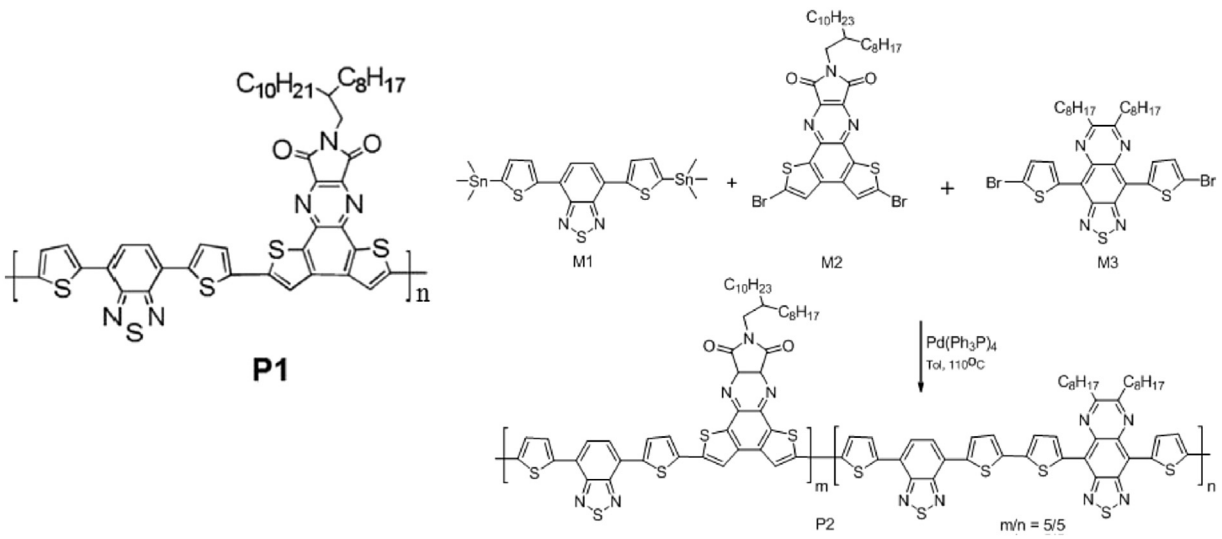

Scheme 1. Synthesis routes of **P2** and chemical structure of **P1** is also shown.

methanol. Finally, the precipitate was collected and dried under vacuum overnight to get polymer **P2** as dark brown solid. Yield (0.348 g, 79%).^{1}H NMR (400 MHz, $CDCl_3$, δ ppm): 8.30–7.00 (m, 18 H), 5.50–4.00 (m, 6 H), 2.90–0.50 (m, 69 H). Elem. Anal. For $(C_{94}H_{94}N_{11}S_{11}O_2)_n$. Calc: C, 64.06; H, 5.38; N, 8.74; S, 20.01. Found: C, 63.07; H, 4.40; N, 7.99; S, 19.24.

4. Device fabrication and characterization

The PSCs were fabricated on glass substrates patterned with indium tin oxide (ITO) with resistivity of 10 Ω sq^{-1} with a conventional structure ITO/PEDOT:PSS (40 nm)/active layer (90 nm ± 5 nm)/PFN (20 nm)/Al. The ITO patterned glass was cleaned sequentially with detergent, deionized water, acetone and isopropyl alcohol using ultrasonication for 10 min each. After drying in a vacuum oven at 50 °C for 12 h, the substrates were treated with UV-ozone for 30 min. The poly-(3,4-ethylenedioxythiophene): poly(styrene sulfonic acid) (PEDOT: PSS, VP AI 4083, Clevious) (~40 nm) was spin coated on clean ITO substrates at 3500 rpm for 30 s as a hole transport layer and then annealed at 110 °C for 10 min in air. The thickness of the PEDOT:PSS was measured using a surface profiler. An active layer solution mixture of the terpolymer (**P2**) and $PC_{71}BM$ (different weight ratios) (total concentration of 18 mg/mL) in the di-chlorobenzene (DCB) solvent with or without 1,8-diiodooctane (DIO) was prepared, which was then spin-coated onto the PEDOT: PSS layer in ambient conditions and dried at 50 °C for 2 h in order to remove the solvent residue. . A methanol solution of PFN with concentration of 1.5 mg/mL was then spin coated onto the top of the photoactive layer at 3000 rpm for 30 s and dried in a vacuum oven for 2 h. Finally, aluminum (Al) top electrode was deposited onto the top of PFN buffer layer by thermal evaporation at a base pressure of 1 × 10^{-5} Pa through a shadow mask area of 20 mm^2.

The current-voltage characteristics of the devices were measured using a computer-controlled Keithley 2400 source meter under stimulated AM1.5 G at an intensity of 100 mW/cm^2 provided by a solar simulator. The incident photon to current efficiency (IPCE) of the devices was measured by illuminating the device through the light source and the monochromator and the resulting current was measured using a Keithley electrometer under short circuit conditions. The hole mobilities of the active layers were determined by fitting the dark current to the model of space charge limited current (SCLC) in the hole only device with the configuration ITO/PEDOT:PSS/active layer/Au. The active layers were deposited under the same conditions as for the corresponding solar cells.

5. Results and discussion

5.1. Synthesis of polymers

The synthetic routes to the random terpolymer **P2** is shown in Scheme 1. The monomers **M1** (4,7-bis[5-(trimethylstannyl)thiophen-2-yl]-2,1,3-benzothiadiazole) [11], **M2** (2,5-dibromo-9-(2-octyldodecyl)-8*H*-pyrrolo[3,4-b]bisthieno[2,3-f:3′,2′–h]quinoxaline-8,10(9*H*)-dione (PTQD) [12], **M3** (4,9-bis(5-bromithiophen-2-yl)-6,7-bis(2-ethylhexyl) [1,2,5]thiadiazolo[3,4-g]quinoxaline) [13] in Scheme 1, were synthesized according to the procedure reported in the literature. New random terpolymer **P2** was prepared by the Stille copolymerization of monomer **M1** with monomers **M2** and **M3**. The polymerization was carried out under the Stille cross-coupling conditions of three monomers (Scheme 1). Resulting polymer was purified by Soxhlet extraction with methanol, hexane, acetone, and chloroform. The random terpolymer **P2** was obtained by precipitation from the chloroform fraction and the yield is about 79%. **P2** was characterized by ^{1}H NMR spectroscopy (as shown in Fig. 1) and elemental analysis. The elemental analysis data of the

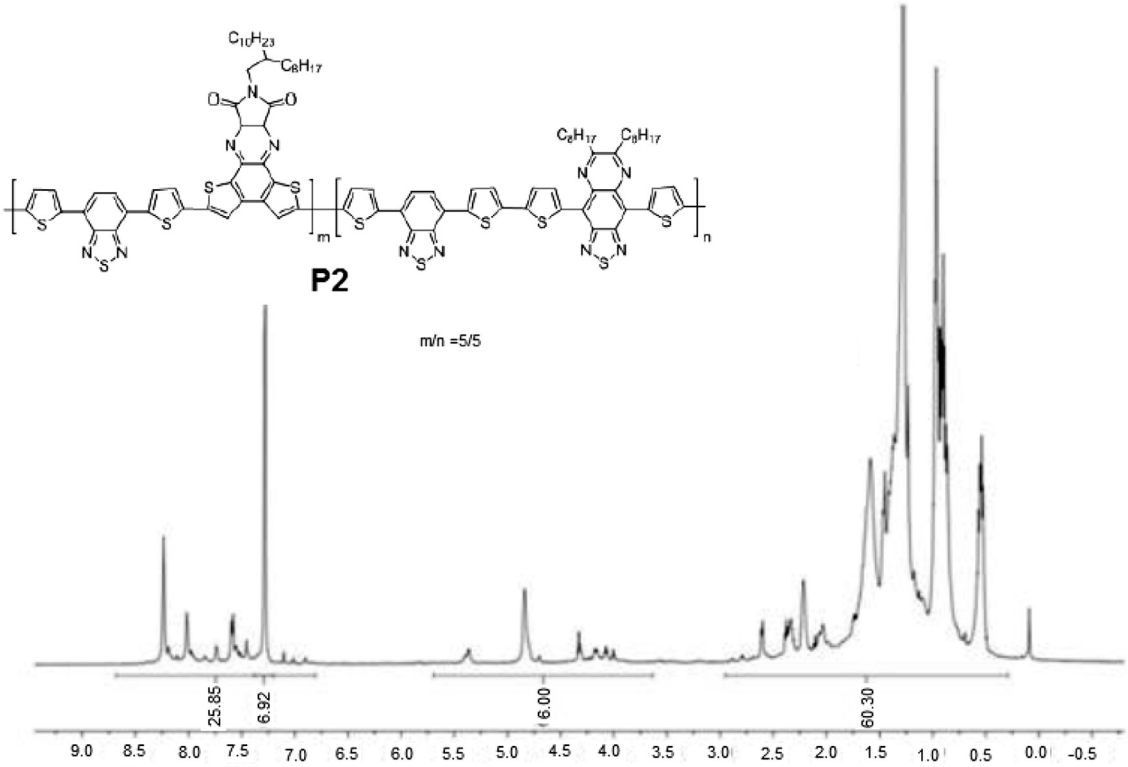

Fig. 1. ^{1}H NMR spectra of random terpolymer **P2** in $CDCl_3$ solution.

polymer match well with theoretical values with a discrepancy of 1–2%, confirms that the copolymer is related to monomers in feed, even with small discrepancy of elemental analysis. Sometimes it is very difficult to dry traces of residual solvents of the polymers and it could make discrepancy between the theoretical and experimental values. The copolymer possesses good solubility in common organic solvents such as chloroform, chlorobenzene, and *o*-dichlorobenzene. The number-average molecular weights (M_n) and polydispersity indexes (PDIs) of the polymer were determined by gel permeation chromatography (GPC) analysis with a polystyrene calibration standard and chloroform as the eluent. The number-average molecular weights (M_n) of the terpolymer **P2** is around 16.1 kDa, and the PDI is 1.90, whereas the M_n and PDI for **P1** are 13.5 kDa and 2.90, respectively.

5.2. Thermal properties

Thermal properties of the polymer were investigated by thermogravimetric analysis (TGA) and differential scanning calorimetry (DSC) and the corresponding data are collected in Table 1. The TGA plots (Fig. 2a) revealed that the decomposition temperature (T_d) values of **P2** (5%weight loss) is 385 °C which is almost same as **P1**. Obviously, terpolymer exhibited excellent thermal stability, which is important for their applications in PSCs and other optoelectronic devices. There are no apparent thermal transitions between 0 °C and 300° C in the second heating and cooling DSC scans terpolymer **P2** (Fig. 2b).

5.3. Optical properties

The optical properties of the random terpolymer **P2** in DCB solution and thin films are shown in Fig. 3. The detailed absorption data, including the absorption maxima wave lengths (λ_{max}) in both solution and film and optical bandgap (E_g^{opt}), are summarized in Table 2 along with the parent polymer **P1**. In solution **P2** displayed broad absorption bands in the range of 350–1100 with two strong characteristic absorption bands at 350–500 nm (centered as 380 nm) and 550–1100 nm (centered at 547 nm). The absorption band in the shorter wavelength region is assigned to delocalized excitonic π-π* transition, while the longer wavelength band with a vibronic absorption shoulder in the wavelength 550–1200 nm is attributed to intramolecular charge transfer interactions between donor and acceptor units in the terpolymer. Similar to the absorption in solution the **P2** film cast from the DCB solution shows to absorption peaks at 380 nm and 560 nm. The absorption band in longer wavelength region has red-shifted also gets broadened as compared to solution, suggesting the presence of intermolecular interactions and aggregation of polymer chain, in solid state. The absorption maxima and band gap values **P2** in thin films are included in Table 1 along with those for parent polymer **P1** for comparison. On introduction of **M3** units into terpolymer **P2** the absorption spectrum is red-shifted, both in solution and in the solid state, and E_g^{opt} value is decreased, suggesting that **M3** units contribute to the expansion of the absorption range of the **M3** based copolymer, which is expected to increase the short-circuit density (J_{sc}) of the PSC device. Generally, the incorporation of electron accepting groups reduces the optical bandgap by raising the energy level of HOMO.

In the solid films the absorption maxima of the polymer film red shifted in comparison with their absorption maxima in solution, caused by a certain extent aggregation of polymer backbone and intermolecular interactions in solid state. Comparing to the parent copolymer **P1** the broad absorption of P2 was observed from 350 to 1200 nm, indicating that the incorporation of two different electron-deficient units into polymer backbone is an effective method to broaden the absorption band and control the optical band gap. Compared to the parent polymer **P1**, the terpolymer **P2** displays a significantly broad absorption covering the wavelength range of 350–1200 nm. The optical bandgap (E_g^{opt}) of is 1.50 and 1.18 eV for **P1** and **P2**, respectively, calculated from the absorption edges (λ_{edge}) of solid state films (Table 2). This indicates that the incorporation of a **M3** unit in the **P2** main chain reduces the band gap significantly. Obviously, random terpolymer **P2** exhibit lower bandgaps than the parent polymer **P1** because of the introduction of **M3** unit into polymer main chains. The results show that broad absorptions of the random terpolymers can be achieved by regulating the composition of the electron-deficient units. The results clearly indicate that incorporation of two different electron-deficient units into polymer backbone is an effective method to broaden the absorption band and to tailor the optical bandgap.

5.4. Electrochemical properties

To estimate the highest occupied/lowest unoccupied molecular orbital (HOMO/LUMO) energy levels of **P1** and **P2**, via cyclic voltammetry (CV) measurements were performed in a three electrode electrochemical system. The polymer cast film on a platinum working electrode was immersed in an acetonitrile solution containing 0.1 M *tetra*-butylammoniumtetrafluoroborate (Bu_4NBF_4), Ag/AgCl as a reference electrode and platinum wire as a counter electrode. The solution was purged with nitrogen for 2 min and then the measurements were performed. The CV curve of terpolymer **P2** is shown in Fig. 4. Before CV analysis, the instrument was calibrated with the common ferrocene/ferrocenium ion (Fc/Fc^+) standard. The HOMO and LUMO energy levels of **P2** are summarized in Table 2 along with those of **P1** for comparison. The HOMO/LUMO energy levels of **P1** and **P2** were calculated to be-5.44/-3.84 eV and −5.10/3.83 eV, respectively. The electrochemical band gaps of **P1** and **P2** were estimated to be 1.60 eV and 1.27 eV, respectively and those are found to be larger than the optical band gap. The LUMO energy level of **P1** and **P2** are almost same, but HOMO energy levels are different, attributed to the same donor unit and different acceptor units in the **P1** and **P2** backbone, since the HOMO and LUMO energy levels of D-A conjugated copolymers are decided by the donor and acceptor units, respectively. In addition, the LUMO levels of the **P2** were at least ≈0.37eV higher than the LUMO level of $PC_{71}BM$, which is expected to be ideal energy difference for efficient electron transfer from the **P2** to $PC_{71}BM$.

5.5. Photovoltaic properties

The photovoltaic properties of **P2** were investigated with a device structure of ITO/PEDOT:PSS/**P2**:$PC_{71}BM$/PFN/Al under illumination intensity of AM1.5 G at 100 mW/cm^2. The fabrication conditions such as weight ratio of **P2** to $PC_{71}BM$ and amount of 1, 8-diiodooctane (DIO) additive in host DCB solution were optimized. The optimal weight ratio between **P2** and $PC_{71}BM$ for optimized active layer is 1:2. The *J-V* characteristics of the PSCs under illumination (AM1.5G, 100 mW/cm^2) are shown in Fig. 5a and the

Table 1
Molecular weights and thermal properties of polymers **P1** and **P2**.

Polymer	Yield (%)	M_n[a] (kDa)	M_w (kDa)	PDI	T_d[b] (°C)
P2	79	16.1	30.59	1.90	385
P1	71	13.5	39.15	2.90	385

[a] Determined by GPC in chloroform with polystyrene standards.
[b] Decomposition temperature, determined by TGA in nitrogen based on 5% weight loss.

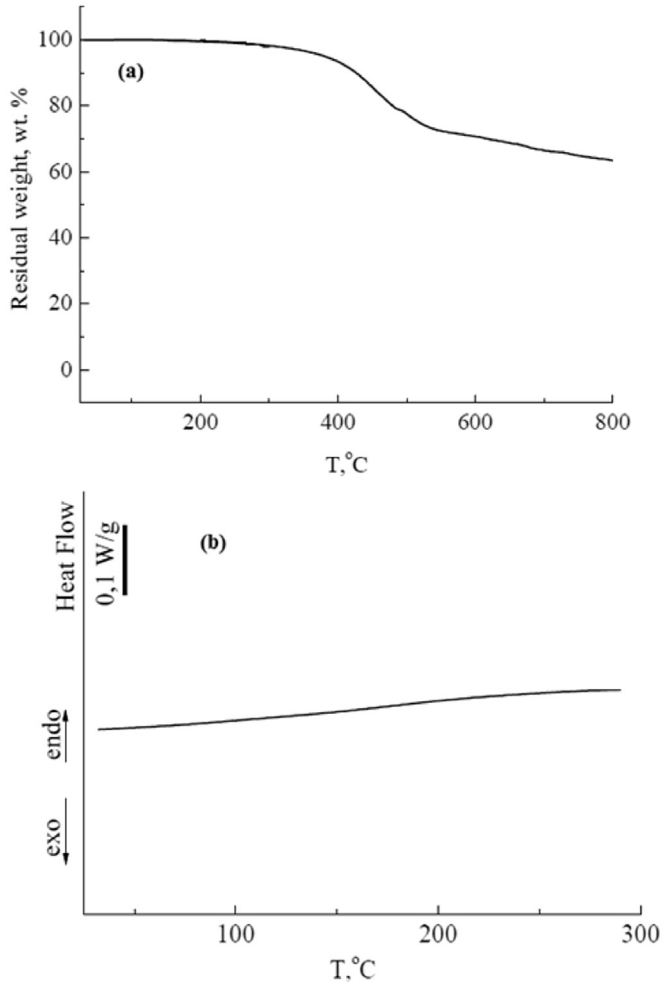

Fig. 2. (a) TGA and (b) DSC plots for **P2** with a heating rate of 10 °C min^{-1} in argon.

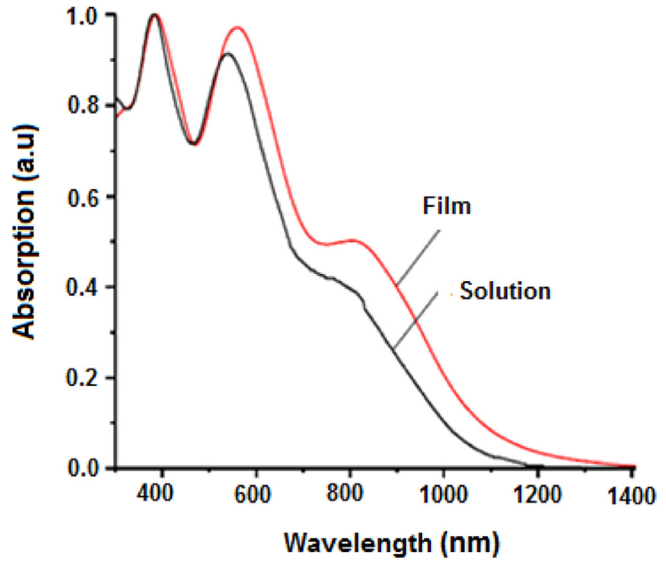

Fig. 3. UV–vis–NIR absorption spectra **P2** in dichlorobenzene solutions and thin film.

photovoltaic parameters were summarized in Table 3. Under the optimized conditions, **P2** based PSCs, processed with DCB, showed

Table 2
Optical and electrochemical properties of **P1** and **P2** in solution and in thin films.

Polymer	λ_{max}^{soln} (nm)	λ_{max}^{film} (nm)	E_g^{opt} (eV)[a]	E_{HOMO}^{ec} (eV)	E_{LUMO}^{ec} (eV)	E_g^{ec} (eV)
P2	380,547	380,560	1.18	−5.10	−3.83	1.27
P1	378, 524	384, 556	1.50	−5.44	−3.84	1.6

[a] Calculated from the absorption band onset of thin film, $E_g^{opt} = 1240/\lambda_{onset}^{film}$.

PCEs of 4.66% (J_{sc} = 10.86 mA/cm^2, V_{oc} = 0.78 V and *FF* = 0.55) which is higher than that for**P1** based PSC (4.40%). The PSCs based on **P2** random terpolymer exhibit higher PCE than that of **P1**, mainly due to the larger values of J_{sc} and *FF*, although the V_{oc} of the device based on **P1** is higher than that of **P2**, is related to the deeper HOMO energy level of **P1** compared to **P2** [14]. The relatively larger value of J_{sc} is mainly related to the broader absorption profile and low optical bandgap of **P2** as compared to **P1**. After the DIO into the active layer solutions, extensively used for improving BHJ morphology [15], the PSCs showed significantly improved device properties. The PCE of the devices significantly improved after the addition of DIO solvent additive, i.e. 7.22% (J_{sc} = 14.12 mA/cm^2, V_{oc} = 0.72 V and *FF* = 0.71) for **P2** which is higher than that for **P1** (6.13%). These observations and results are in good agreement with the IPCE spectra of **P2** based devices (Fig. 5b) obtained with identical conditions. The IPCE spectra of the devices based on **P2**:$PC_{71}BM$ is broader than that for **P1**:$PC_{71}BM$, which is good agreement with the absorption spectra of **P2**. The values of the J_{sc} estimated from the integration of IPCE spectra are collected in Table 3, which were closely matched with the values obtained in the *J-V* characteristics under illumination. After the DIO solvent additive treatment, the V_{oc} slightly decreased, may be the larger energy loss and changes in morphology of the active layer [16].

It can be seen that a high V_{oc} of 0.78–0.72 V was observed for the device based on P2 even the **P2** has a narrow optical bandgap of 1.18 eV [17]. The minimum energy loss (E_{loss}) is defined by the equation: $E_{loss} = E_g - qV_{oc}$, where E_g is the optical bandgap of main light absorber, in most cases the donor material. Decreasing the E_{loss} will enhance the V_{oc} and thus PCE of PSCs [17]. Interesting, the E_{loss} for PSCs based on **P2** is only 0.46eV, far less than the previously suggested minimum value of 0.6 eV [18] but very close to recently reported in literature [19]. Recently, it was reported that PSC based on a low bandgap polymer consist of naphthobisoxadiazole acceptor unit, attains a PCE of 8.9% with E_{loss} below 0.6 eV [20]. We have measured the average dielectric constant of **P1** and **P2** at 100 kHz is 3.53 and 3.86, respectively. The dielectric constant of 3.86 is higher than those of common conjugated polymers, suggesting larger dielectric constant can effectively reduce the E_{loss} in the PSCs. The PCE of 7.22% is one of the highest values of PSCs using a low bandgap terpolymer.

In order to investigate the effect of different acceptors in the terpolymers and additive on the charge carrier mobility of the active layer, hole only devices with a structure of ITO/PEODT:PSS/active layer/Au and electron only devices with configuration glass/Al/active layer/Al were fabricated. The hole mobility (μ_h) and electron mobility (μ_e) of the active layers were measured from the dark *J-V* characteristics by space charge limited current (SCLC) model. The *J-V* characteristics of the hole only device based on **P2**:$PC_{71}BM$ active layer processed with and without DIO are shown in Fig. 6. Similar *J-V* characteristics were also observed for electron only devices. The μ_h for **P1**:$PC_{71}BM$ and **P2**:$PC_{71}BM$ active layers without DIO additive are 1.56 × 10^{-5} cm^2/V [10] and 3.21 × 10^{-5} cm^2/V, respectively, whereas μ_e for **P1**:$PC_{71}BM$ and **P2**:$PC_{71}BM$ are about 2.46 × 10^{-4} and 2.58 × 10^{-4} cm^2/V, respectively. The higher value of μ_h of **P2**:$PC_{71}BM$ active layer also confirm the higher values of J_{sc} and *FF*. When the active layers are processed

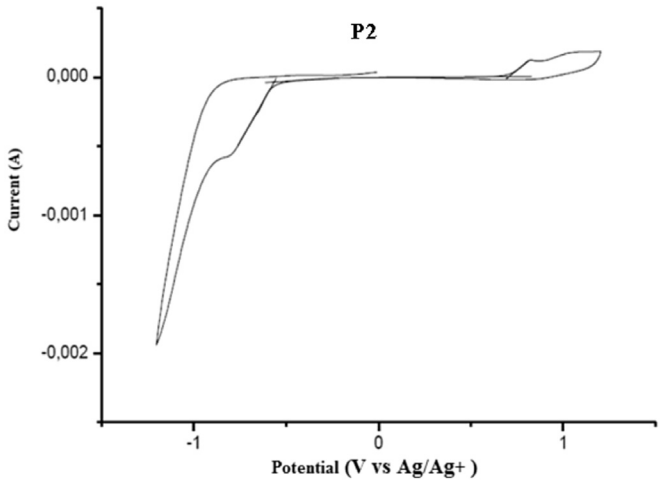

Fig. 4. CV of **P2** film casted on platinum working electrode in 0.1M Bu_4NPF_6/acetonitrile at 100 mV/s, potential vs Ag/Ag+.

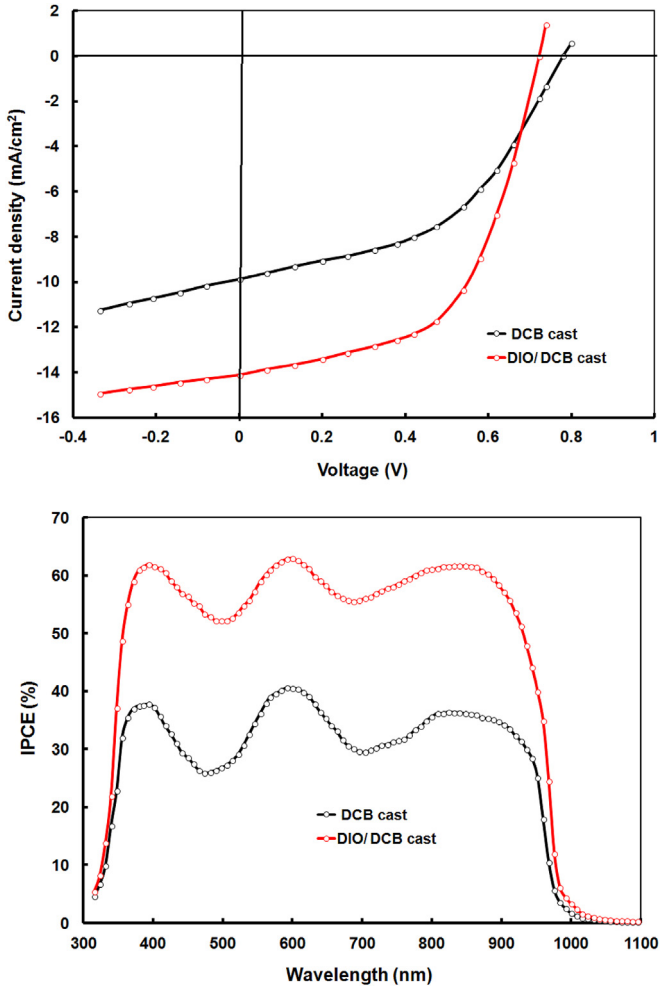

Fig. 5. (a) Current-voltage (J–V) characteristics under illumination and (b) IPCE spectra of the devices based on **P2**:$PC_{71}BM$ processed with and without DIO additives.

with DIO additive, the μ_h for **P1**:$PC_{71}BM$ and **P2**:$PC_{71}BM$ was increased up to 2.16 × 10^{-4} cm^2/V and 1.48 × 10^{-4} cm^2/V, respectively whereas the μ_e is almost remain unchanged. The use of

Table 3
Photovoltaic parameters of the PSCs based on **P1** and **P2**.

Active layer	J_{sc} (mA/cm^2)	V_{oc} (V)	*FF*	PCE (%)	J_{sc}(mA/cm^2)[c]
P2:$PC_{71}BM$[a]	10.86	0.78	0.55	4.66	10.75
P2:$PC_{71}BM$[b]	14.12	0.72	0.71	7.22	14.03
P1:$PC_{71}BM$[d]	9.26	0.88	0.54	4.40	9.04
P1:$PC_{71}BM$[d]	11.92	0.86	0.64	6.56	11.52

[a] DCB cast.
[b] DIO/DCB cast.
[c] Estimated from IPCE spectra.
[d] Our earlier work Ref [10].

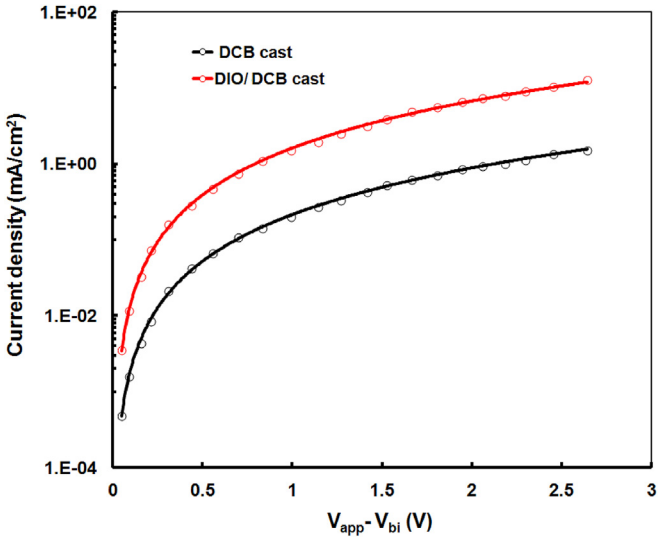

Fig. 6. Current-voltage plots of hole only devices processed with and without DIO additives. Solid lines represent the SCLC fitting.

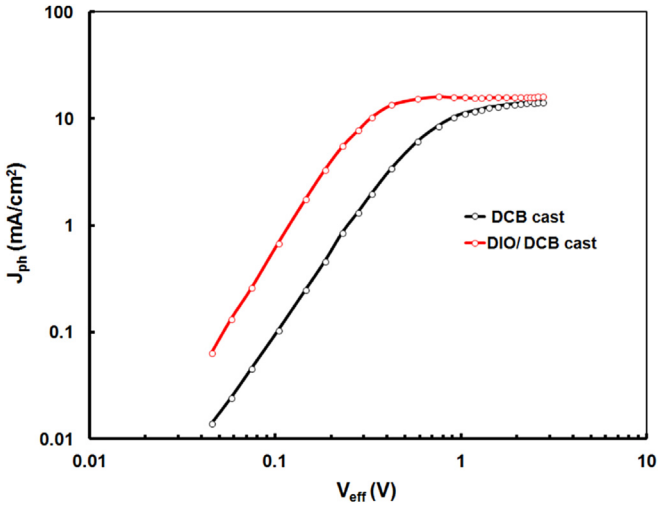

Fig. 7. Variation of photocurrent (J_{ph}) with effective voltage (V_{eff}) for the devices based on **P2**:$PC_{71}BM$ processed with DCB and DIO/DCB solution.

DIO additive could promote the aggregation of terpolymers in the blended films which is beneficial to the hole transport. The enhancement in the μ_h led to a more balanced hole and electron mobility, resulting higher J_{sc} and *FF* [21].

In order to explain the reason for the high J_{sc} for PSC based on **P2**:$PC_{71}BM$ processed with and without DIO, we calculated and compared the exciton generation rates (G_{max}) of the blended films

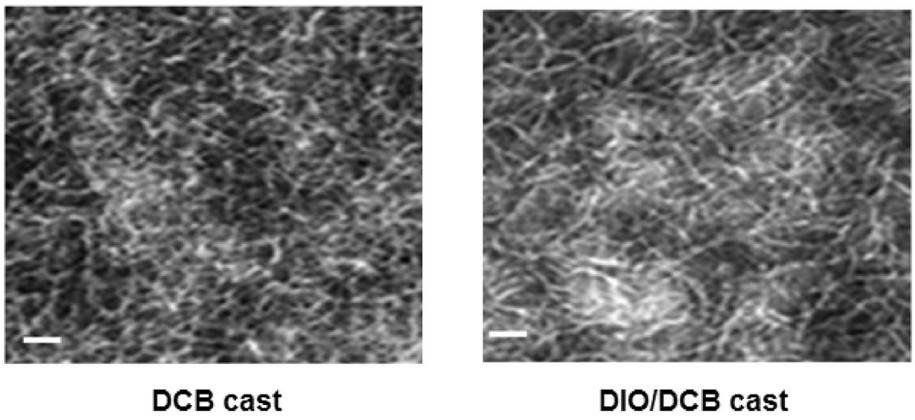

Fig. 8. Transmission electron microscopy (TEM) images of **P2**:$PC_{71}BM$ thin films cast from DCB and DIO/DCB.

[22]. The G_{max} was estimated by plotting the photocurrent density (J_{ph}, defined as J_L-J_D, where J_L and J_D are the current density under illumination and in the dark, respectively) as a function of effective voltage (V_{eff}, defined as V_o- V_{appl}, where V_o is the voltage where J_{ph} is zero and V_{appl} is the applied voltage). Comparison of G_{max} values revealed that G_{max} value of PSC with **P2**:$PC_{71}BM$ processed with DIO (1.17×10^{28} $m^{-3}s^{-1}$) is higher than that of as cast (1.03×10^{28} $m^{-3}s^{-1}$). These values are higher than that for **P1**:$PC_{71}BM$ based devices. Therefore, we conclude that the high value of J_{sc} of **P2** based PSC arises high charge generation probability due to the broad photon absorption in 660–1100 nm. It can be seen from Fig. 7, the photocurrent of the device based on as cast **P2**:$PC_{71}BM$ starts saturated at higher value of V_{eff}, indicating that charge recombination is occurring in this device. For device based on DIO/DCB processed **P2**:$PC_{71}BM$, the photocurrent starts saturating at low bias voltages and reaches full saturation at 2.8 V, demonstrating that the photogenerated excitons in this device were fully dissociated and the free charge carriers were effectively transported within the active layer and then collected by the anode and cathode electrodes. Moreover, the exciton dissociation probability (P_c) was also estimated from $P_c = J_{sc}/J_{phsat}$ for the devices. If the P_c is 100%, then the germinate recombination loss of charge carriers is negligible. Since only a fraction of photogenerated excitons are able to dissociate into free charge carriers at donor/acceptor interface and also depends upon the morphology of the active layer used in the devices. The values of P_c for **P2**:$PC_{71}BM$ active layer processed with and without DIO are 88% and 76%, respectively. The lower value of **P2**:$PC_{71}BM$ strongly indicated that relatively large fraction of excitons recombine before the charge separation.

Both the blended film showed well defined interconnected network structure as shown in TEM images (Fig. 8). The **P2**:$PC_{71}BM$ blend film cast from DCB showed slightly poor phase separation, may suppress charge transport after the exciton dissociation at donor/acceptor interface, therefore showed low value of J_{sc} than **P2**:$PC_{71}BM$ processed with DIO/DCB. The formation of aggregation by the terpolymers after DIO additive could enhance the hole mobility in the blended films which beneficial to the enhancement of J_{sc}.

6. Conclusions

A random terpolymer **P2** with same thiophene donor and different accepting units was successfully designed and its optical and electrochemical properties were investigated in order to employ them as electron donor for solution processed bulk heterojunction polymer solar cells. The **P2** (1.18 eV) showed significantly low optical bandgap as compared to parent polymer **P1** (1.50 eV). After the optimization of active layers (weight ratio between **P2** and $PC_{71}BM$ and concentration of solvent additive), PSC based on **P2** shows a conversion efficiency of 7.22% which is higher than that for **P1** (6.56%). Improved photo-absorption and charge carriers mobility due to the extended conjugation and efficient ordering of conjugated terpolymer are most likely the cause of high PCE of PSC. Moreover PCE of 7.22% with a low bandgap polymer (1.18 eV) is achieved by may be the highest PCE with our best of knowledge.

Acknowledgements

M.L.K. N.A.R., S.A.K thanks Russian Science Foundation (grant number 14-13-01444).

References

[1] (a) L. Dou, J. You, Z. Hong, Z. Xu, G. Li, R.A. Street, Y. Yang, Adv. Mater 25 (2013) 6642–6671;
(b) K.A. Mazzio, C.K. Luscombe, Chem. Soc. Rev. 44 (2015) 78–90;
(c) J.-S. Wu, S.-W. Cheng, Y.-J. Cheng, C.-S. Hsu, Chem. Soc. Rev. 44 (2015) 1113–1154;
(d) L. Lu, T. Zheng, Q. Wu, A.M. Schneider, D. Zhao, L. Yu, Chem. Rev. 115 (2015) 12666–12731;
(e) L. dou, Y. Liu, Z. Hong, G. Li, Y. Yang, Chem. Rev. 115 (2015) 12633–12665.
H. Yao, L. Ye, H. Zhang, S. Li, S. Zhang, J. Hou, Chem. Rev. 116(2016) 7397–7457.
[2] (a) Z. He, B. Xiao, f. Liu, H. Wu, Y. Yang, S. Xiao, C. Wang, T.P. Russell, Y. Cao, Nat. Photonics 2015 (9) (2015) 174–179;
(b) J. Zhao, Y. Li, G. Yang, K. Jiang, H. Lin, H. Ade, W. Ma, H. Yan, Nat. Energy 1 (2016) 15027;
(c) S. Zhang, L. Ye, J. Hou, Adv. Energy Mater. (2016), http://dx.doi.org/10.1002/aenm.20502529;
(d) V. Vohra, K. Kawashima, T. Kakara, T. Koganezawa, I. Osaka, K. Takimiya, H. Murata, Nat. Photonics 9 (2015) 403–408;
(e) Y. Liu, J. Zhao, Z. Li, C. Mu, W. Ma, H. Hu, K. Jiang, H. Lin, H. Ade, H. Yan, Nat. Commun. 5 (2014) 5293;
(f) W. Zhao, D. Qian, S. Zhang, S. Li, O. Inganas, F. Gao, J. Hou, Adv. Mater. 28 (2016) 4734–4739;
(g) S. Liu, P. You, J. Li, J. Li, C.-S. Lee, B.S. Ong, C. Surya, F. Yan, Energy Environ. Sci. 8 (2015) 1463–1470;
(h) C. Liu, C. Yi, K. Wang, Y. Yang, R.S. Bhatta, M. Tsige, S. Xiao, X. Gong, ACS Appl. Mater. Interfaces 7 (2015) 4928–4935;
(i) H. Zhou, Y. Zhang, C.K. Mai, S.D. Collins, G.C. Bazan, T.Q. Nguyen, A.J. Heeger, Adv. Mater. 27 (2015) 1767–1773;
(j) F. Huang, Sci. China Chem. 58 (2015) 190.
[3] (a) B. Xiao, G. Ding, Z. Tan, E. Zhou, Poly. Chem. 6 (2015) 7594–7602;
(b) M.C. Yuan, M.Y. Chiu, C.M. Chiang, K.H. Wei, Macromolecules 43 (2010) 6270.
[4] (a) J. Zhou, S. Xie, E.F. Amond, M.L. Becker, Macromolecules 46 (2013) 3391–3394;
(b) J.W. Jung, F. Liu, T.P. Russell, W.H. Jo, Energy Environ. Sci. 6 (2013) 3301–3307.

[5] (a) T.E. Kang, K.H. Kim, B.J. Kim, J. Mater. Chem. A 2 (2014) 15252–15267;
(b) T. Qin, W. Zajaczkowski, W. Pisula, M. Baumgarten, M. Chen, M. Gao, G. Wilson, C.D. Easton, K. Mullen, S.E. Watkins, J. Am. Chem. Soc. 136 (2014) 6049–6055.
[6] (a) V. Tamilavan, K.H. Roh, R. Agneeswari, D.Y. Lee, S. Cho, Y. Jin, S.H. Park, M.H. Hyun, J. Mater. Chem. A 2 (2014) 20126–20132;
(b) I.E. Kuznetsov, A.V. Akkuratow, D.K. Susarova, D.V. Anokhin, Y.L. Moskvin, M.V. Kluyev, A.S. Peregudov, P.A. Troshin, Chem. Commun. 51 (2015) 7562–7564;
(c) J.H. Kim, H.U. Kim, I.N. Kang, S.K. Lee, S.J. Moon, W.S. Shin, D.H. Hwang, Macromolecules 45 (2012) 8628–8638;
(d) H. Li, F. Liu, X. Wang, C. Gu, P. Wang, H. Fu, Macromolecules 46 (2013) 9211–9219;
(e) K.H. Kim, S. Park, H. Yu, H. Kang, I. Song, J.H. Oh, B. Kim, J. Chem. Mater. 26 (2014) 6963–6970.
[7] E. Zhou, J. Cong, K. Hashimoto, K. Tajima, Energy Environ. Sci. 5 (2012) 9756–9759.
[8] J.W. Lee, H. Ahn, W.H. Jo, Macromolecules 48 (2015) 7836–7842.
[9] Y.S. Lee, J.Y. Lee, S.M. Bang, B. Lim, J. Lee, S.I. Na, J. Mater. Chem. A 24 (2016) 11439–11445.
[10] M.L. Keshtov, S.A. Kuklin, D.Y. Godovsky, A.R. Khokhlov, R. Kurchania, F.C. Chen, Emmanuel N. Koukaras, G.D. Sharma, J. Poly. Sci. Part A Poly Chem. 54 (2016) 155–168.
[11] M.C. Scharber, D. Muhlbacher, M. Koppe, P. Denk, C. Waldauf, A.J. Heeger, C.J. Brabec, Adv. Mater 18 (2006) 789–794.
[12] M.L. Keshtov, S.A. Kuklin, F.C. Chen, A.R. Khokhlov, RajnishKurchania, G.D. Sharma, J. Polym. Sci. Polym. Chem. 53 (2015) 2390–2398.
[13] M.L. Keshtov, D.V. Marochkin, V.S. Kochurov, A.R. Khokhlov, E.N. Koukaras, G.D. Sharma, Polym. Chem. 2013 (4) (2013) 4033–4044.
[14] G. Dennler, M.C. Scharber, C.J. Brabec, Adv. Mater. 21 (2009) 1323–1338.
[15] (a) J.K. Lee, W.L. Ma, C.J. Brabec, J. Yuen, J.S. Moon, J.Y. Kim, K. Lee, G.C. Bazan, A.J. Heeger, J. Am. Chem. Soc. 130 (2008) 3619–3623;
(b) X. Guo, C. Cui, M. Zhang, L. Huo, Y. Huang, J. Hou, Y. Li, Energy Environ. Sci. 5 (2012) 7943–7949.
[16] (a) M. Wang, H. Wang, T. Yokoyama, X. Liu, Y. Huang, Y. Zhang, T.-Q. Nguyen, S. Aramaki, G.C. Bazan, J. Am. Chem. Soc. 136 (2014) 12576–12579;
(b) W. Li, K.H. Hendriks, A. Furlan, M.M. Wienk, R.A.J. Janssen, J. Am. Chem. Soc. 137 (2015) 2231–2234;
(c) K. Gao, L. Li, T. Lai, L. Xiao, Y. Huang, F. Huang, J. Peng, Y. Cao, F. Liu, T.P. Russell, R.A.J. Janssen, X. Peng, J. Am. Chem. Soc. 137 (2015) 7282–7285.
[17] (a) D. Veldman, S.C.J. Meskers, R.A.J. Janssen, Adv. Funct. Mater. 19 (2009) 1939–1948;
(b) C. Wang, X. Xu, W. Zhang, J. Bergvist, Y. Xia, X. Meng, K. Bini, W. Ma, A. Yartserv, K. Vandewal, M.R. Andersson, O. Inganas, M. Fahlmen, E. Wang, Adv. Energy Mater. 2 (2016) 201600148.
[18] K. Kawashima, Y. Tamai, H. Ohkita, I. Osaka, K. Takimiya, Nat. Commun. 6 (2015) 10085.
[19] C. Lu, H.-C. Chen, W.-T. Chuang, Y.-H. Hsu, W.-C. Chen, P.-T. Chou, Chem. Mater. 27 (2015) 6837–6847.
[20] B. Qi, J. Wang, Phys. Chem. Chem. Phys. 15 (2013) 8972–8982.
[21] (a) L. Lu, Z. Luo, T. Xu, L. Yu, Nano Lett. 13 (2013) 59–64;
(b) J.W. Lee, S. Bae, W.H. Jo, J. Mater. Chem. A 2 (2014) 14146–14153;
(c) L. Lu, T. Zheng, T. Xu, D. Zhao, L. Yu, Chem. Mater 27 (2015) 537–543.